Biochemical and Biophysical Research Communications 582 (2021) 86–92

Contents lists available at ScienceDirect

Biochemical and Biophysical Research Communications

journal homepage: www.elsevier.com/locate/ybbrc

Crystal structure of yeast Gid10 in complex with Pro/N-degron

Jin Seok Shin, Si Hoon Park, Leehyeon Kim, Jiwon Heo, Hyun Kyu Song*

Department of Life Sciences, Korea University, 145 Anam-ro, Seongbuk-gu, Seoul, 02841, South Korea

ARTICLE INFO

Article history:
Received 30 September 2021
Accepted 3 October 2021

Keywords:
E3 ubiquitin ligase
GID complex
N-degron
Proline
Saccharomyces cerevisiae
X-ray crystallography

ABSTRACT

The cellular glucose level has to be tightly regulated by a variety of cellular processes. One of them is the degradation of gluconeogenic enzymes such as Fbp1, Icl1, Mdh2, and Pck1 by GID (glucose-induced degradation deficient) E3 ubiquitin ligase. The Gid4 component of the GID ligase complex is responsible for recognizing the N-terminal proline residue of the target substrates under normal conditions. However, an alternative N-recognin Gid10 controls the degradation process under stressed conditions. Although Gid10 shares a high sequence similarity with Gid4, their substrate specificities are quite different. Here, we report the structure of Gid10 from *Saccharomyces cerevisiae* in complex with Pro/N-degron, Pro-Tyr-Ile-Thr, which is almost identical to the sequence of the natural substrate Art2. Although Gid10 shares many structural features with the Gid4 protein from yeast and humans, the current structure explains the unique structural difference for the preference of bulky hydrophobic residue at the second position of Pro/N-degron. Therefore, this study provides a fundamental basis for understanding of the structural diversity and substrate specificity of recognition components in the GID E3 ligase complex involved in the Pro/N-degron pathway.

1. Introduction

Ubiquitin (Ub) plays a role as a critical modulator of many biological processes, including the cell cycle, signal transduction, DNA transcription, autophagy, and proteasomal degradation [1–3]. The ubiquitin–proteasome system (UPS) is a conserved pathway for degrading proteins in a highly regulated manner in eukaryotic cells [1,4]. In addition to Ub and the proteasome, the UPS consists of many factors, including three different sets of enzymes, E1 Ub-activating enzymes, E2 Ub-conjugating enzymes, and E3 Ub ligases. In particular, E3 Ub ligases play a critical role in recognizing the substrate and eventually linking Ub from the E2 enzyme to the target protein [5]. Diverse combinations of E2 Ub-conjugating enzymes and E3 Ub ligases recognize each substrate's distinctive degradation signal, thereby yielding delicate specificity for ubiquitylation of various protein substrates [6]. Consequently, Ub-tagged substrates are degraded by the 26S proteasome, and eukaryotic cells can maintain homeostasis by selectively eliminating misfolded, damaged, and metabolically unwanted proteins [1,2].

One of the degradation signals is N-degron, which is recognized by E3 ligases called N-recognins, and the proteolytic system is termed the N-degron pathway (formerly called the N-end rule pathway) [6]. The Arg/N-degron pathway targets unacetylated N-terminal (Nt) residues containing Asn, Arg, Asp, Cys, Gln, Glu, His, Ile, Leu, Lys, Met, Phe, Trp, and Tyr [6,7]. Some of them are modified to Nt-Arg by successive hierarchical enzymatic processes [6,8]. The Ac/N-degron pathway, an alternative pathway of Arg/N-degron, targets proteins bearing acetylated Nt-residues containing Ala, Cys, Gly, Met, Ser, Thr, and Val, although some of them are rarely acetylated [6,9]. More recently, the Gly/N-degron and fMet/N-degron pathways have been reported to target the Nt-glycine and Nt-formyl methionine residues, respectively [10,11]. Nt-proline has a characteristic cyclic form of side chain and is targeted by the Pro/N-degron pathway involved in the destruction of gluconeogenic enzymes [12].

Gluconeogenesis is a metabolic pathway for generating glucose from noncarbohydrate substances, and it is a ubiquitous metabolic process that exists in almost all living organisms. In *Saccharomyces cerevisiae*, cells switch from gluconeogenesis to glycolysis to maintain an appropriate level of glucose [13–15]. Glucose-induced degradation-deficient (GID) Ub ligase complexes, composed of 9 subunits (Gid1~9), degrade gluconeogenic enzymes when cells return to glucose-replete conditions [16]. The gluconeogenic enzymes Fbp1, Icl1, Mdh2, and Pck1 bearing Nt-Pro or Pro at the second position are conditionally degraded in a Gid4-dependent

* Corresponding author.
E-mail address: hksong@korea.ac.kr (H.K. Song).

https://doi.org/10.1016/j.bbrc.2021.10.007
0006-291X/

manner [12]. Thus, the Gid4 subunit is a recognition component in the GID complex. A follow-up study using yeast-two-hybrid screening identified an alternative recognition component, Gid10 (YGR066C), which shares a degree of substrate specificity with Gid4 but is not identical [17]. Gid10 from *Saccharomyces cerevisiae* (yGid10) is induced under starvation or osmotic stress conditions, and it is interchangeable with Gid4 to be assembled into a GID complex [18]. The recognition specificity of Gid4 from *Saccharomyces cerevisiae* (yGid4) was quite mysterious due to the substrate Pck1, which bears Nt-Ser immediately after the initiating methionine residue, whereas most of the substrates possess proline at the Nt, removing the initiating methionine residue by methionine aminopeptidase(s). Interestingly, the Pro-Thr-Leu-Val sequence derived from a known yGid4 target substrate, Fbp1, interacts extremely weakly with yGid10. Furthermore, yGid10 also recognizes nonproline residues such as Met-Tyr-Ile-Thr-Val or Val-Cys-Phe-His [17]. More recently, it has also been reported that human GID4 (hGID4) recognizes nonproline Nt-residues starting with Ile or Val followed by glycine residues [19].

Structures of hGID4 in complex with Pro/N-degron as well as nonproline peptides have been reported, and therefore, the specificity of hGID4 is relatively well understood [19,20]. In contrast to yGid4, hGID4 has been shown to not bind to the Nt-Ser-Pro-peptide *in vitro* [20]. The cryo-electron microscopy structure of the entire yeast GID complex containing apo-Gid4 has been reported [18], and no structural information on yGid10 has been reported. Therefore, we initiated this study to determine the complex structure of yGid10 in complex with Nt-Ser-Pro N-degron to understand how yGid10 recognizes the Nt-serine residue and the unique specificity of yGid10 [17]. Here, the structure of yGid10 in complex with Pro/N-degron was determined using X-ray crystallography, and it shows similarity as well as unique features compared with yGid4 and hGID4. The structure reveals that the bound peptide is Nt-Pro after processing the Nt-serine residue by aminopeptidase P activity in *E. coli* and the preference of a bulky hydrophobic residue at the second position of the N-degron. These findings broaden our understanding of the structural diversity and substrate specificity of recognition components in the GID E3 Ub ligase complex.

2. Materials and methods

2.1. Cloning

For efficient expression of target proteins in *E. coli*, we used the codon optimization tool ExpOptimizer (https://www.novoprolabs.com). The DNA encoding yGid10 (residues 73–292) was synthesized (Integrated DNA Technologies) and cloned into the FP-His vector containing a C-terminal His-tag. We inserted the DNA sequence encoding the Met-Ser-Pro-Tyr-Ile-Thr-Val sequence at the N-terminus by the QuikChange site-directed mutagenesis method.

2.2. Protein expression and purification

The recombinant protein was overexpressed in *E. coli* BL21 (DE3) cells (Novagen, 69,450) in a 1 × LB medium. Cells were grown at 37 °C at 180 rpm until the OD_{600} reached 1.0, cooled to 18 °C for 5 min, and treated with 0.5 mM isopropyl β-D-1-thiogalactopyranoside (IPTG) for target protein induction. After IPTG treatment, cells were grown at 18 °C for 18 h and harvested for the following steps. The harvested cells were lysed in sonication buffer (50 mM Tris-HCl pH 8.0, 200 mM NaCl, and 1 mM TCEP [tris(2-carboxyethyl)phosphine]), and the lysate was centrifuged at 35,000×*g* for 1 h.

The supernatant was loaded onto an Ni-NTA affinity column (Cytiva, 29-0510-21), and the eluent was further purified by anion exchange column chromatography using HiTrap Q FastFlow (Cytiva, 17-5156-01). Finally, the sample was passed through Superdex 75 Increase 5/150 GL (Cytiva, 29-1487-21) pre-equilibrated with final buffer (20 mM Tris-HCl pH 7.5, 150 mM NaCl, and 1 mM TCEP).

2.3. Crystallization and structure determination

We crystallized the N-degron-fused yGid10 at 20 °C in sitting drop plates by 1:1 mixing of the protein (2.5 mg/ml) and mother liquor (4.95% (v/v) isopropanol and 0.33 M ammonium citrate/ammonium hydroxide with a pH of 8.5). Crystals were flash-frozen in liquid nitrogen with 25% glycerol as a cryoprotectant in the original mother liquor. Data were collected at the Pohang Accelerator Laboratory (PAL) in Korea. The crystal structure of yGid10 was solved by molecular replacement (MR) with the program PHASER [21] using the structure of hGID4 as a search model (PDB ID: 6CDC) [20]. The model obtained from the MR solution was rebuilt and refined in iterative cycles using Coot [22]. Statistics for collected data and refinement are summarized in Table 1. Structural figures were drawn using PyMOL (www.pymol.org/), and for surface hydrophobic map generation, we used ChimeraX (https://www.cgl.ucsf.edu/chimera/) [23]. Visualization of protein-ligand interactions was performed using LIGPLOT (https://www.ebi.ac.uk/thornton-srv/software/LIGPLOT/). Atomic coordinate and structure factor files have been deposited in the Protein Data Bank under the accession code 7VGW.

2.4. Amino acid sequence alignment and calculation of identity

Amino acid sequences of hGID4, yGid4, and yGid10 were taken from the UNIPROT database (https://www.uniprot.org) and aligned using the multiple sequence alignment tool Clustal Omega (https://www.ebi.ac.uk/Tools/msa/clustalo/). Sequence identity and similarity of the aligned sequences were calculated by Sequence Manipulation Suite (www.bioinformatics.org). Visualization of the aligned result was performed by ESPript (https://espript.ibcp.fr/ESPript/ESPript/).

2.5. DNA and N-terminal amino acid sequencing

The DNA sequences for protein expression were analyzed by Cosmogentech Inc. (Seoul, Korea). For N-terminal amino acid sequencing, the purified yGid10 sample was transferred from SDS–PAGE gel to PVDF membrane (Invitrogen, IB24002). The transferred protein band on the membrane was analyzed with the Edman sequencing technique by EMASS Co. (Seoul, Korea).

3. Results and discussion

3.1. Serendipitously generated Pro/N-degron bound to yGid10

To understand how yGid10 or its sequelog yGid4 recognizes the Pro/N-degron substrate, Pck1 bearing the proline residue at the second position immediately after serine residue [12], we designed the following strategy. Previously, it has been reported that the N-degron residues attached at the Nt region of the target protein generated by the LC3B fusion technique are very useful for the complex structure of the proteins involved in the N-degron pathway [24]. Unfortunately, the ATG4B protease cannot cleave the peptide bond between the C-terminal glycine residue of LC3B and the next proline residue. However, it is known that Nt-methionine is removed by methionine aminopeptidase(s) if the side chains of the penultimate residues have a radius of gyration of 1.29 Å or less, including proline residues [25]. As noted, yGid10 binds the Met-Tyr-Ile-Thr-Val sequence tightly [17], and therefore, we designed

Table 1
Data collection and refinement statistics.

PYIT-yGid10 (PDB ID: 7VGW)	
Data collection	
Beamline	PAL-11C
Space group	$C\,2\,2\,2_1$
Cell dimensions	
a, *b*, *c* (Å)	86.346, 109.913, 147.461
α, β, γ (°)	90, 90, 90
Wavelength (Å)	0.9794
Resolution (Å)	43.17–2.8 (2.85–2.8)[a]
R_{merge}	0.175 (1.447)
$I/\sigma I$	14.9 (1.07)
Completeness (%)	99.52 (99.25)
Redundancy	8.8 (7.7)
Refinement	
Resolution (Å)	2.8
No. reflections	17,555 (1728)
R_{work}/R_{free}	21.0/24.8 (29.8/35.1)
No. atoms	3474
B-factors (Å^2)	72.73
R.m.s deviations	
Bond lengths (Å)	0.003
Bond angles (°)	0.65
Ramachandran plot	
Favored (%)	96.57
Allowed (%)	3.43
Outliers (%)	0

[a] Values in parentheses are for the highest-resolution shell.

a construct bearing Met-Ser-Pro-Tyr-Ile-Thr-Val at the Nt of yGid10 and expected Ser-Pro-Tyr-Ile-Thr-Val-yGid10 as a product.

With this construct, we successfully obtained crystals and determined the structure of yGid10 in complex with the N-degron substrate (see details for Section 3.2); however, the electron density map for the N-degron was quite enigmatic and did not look like the expected Nt-Ser residue. Therefore, we double confirmed the DNA sequence (Fig. S1A) and the N-terminal sequence of the purified N-degron-tagged yGid10 (Fig. S1B). The Edman sequencing result clearly showed Nt-Pro, which suggested that Nt-Ser must be further processed by the unknown aminopeptidase P in *E. coli.*, and Chen et al. very recently reported that the N-terminal serine of yeast Pck1 is trimmed by the aminopeptidase Icp55 to expose the Pro/N-degron [26]. This implies that the mechanism for removing amino acid residues, including serine, before proline to make the Pro/N-degron is evolutionarily conserved between *S. cerevisiae* and *E. coli*. In conclusion, we serendipitously obtained the crystal structure of yGid10 in complex with the Nt-Pro peptide from an adjacent molecule in the crystalline lattice (Fig. 1A).

3.2. Overall structure of yGid10

We determined the complex structure of yGid10-PYTI at a resolution of 2.8 Å (Table 1). There were two molecules in the asymmetric unit, and chain-B was selected for further structural analysis because it showed better electron density of the bound Pro/N-degron than chain-A. The overall structure of yGid10 has a well-conserved antiparallel β-barrel with 9 β-strands (β1-a, β1-b, and β2~β8) with the first (β1) and last (β8) β-strands zipped with hydrogen bonds (Fig. 1B and C). This β-barrel possesses a substrate-binding pocket composed of four loops (L1-L4). The pocket shows negatively charged properties formed by three residues (Gln89, Glu217, and Gln270) (Fig. 1D). On the opposite side of the pocket, there are two loops (L5 and L6) and an accessory domain (AD: residues between β4-and β5-strand) composed of two α-helices (Fig. 1C). The exact role of the AD is currently unknown.

3.3. The Pro/N-degron recognition

The proline peptide is recognized by a deep pocket formed by the four loops of the β-barrel, as shown in hGID4 and yGid4 [18,20]. As noted above, the bound N-degron residue is Nt-Pro1-Tyr2-Ile3-Thr4, which is clearly shown in the electron density map (Fig. 1D). Only the four Nt-residues were found inside of the pocket (Fig. 1E), and the next valine residue from the construct was not involved in the interaction with yGid10, although they also showed apparent electron density, which explains why yGid10 has selectivity against only the first four Nt-residues of its substrates [17].

The α-amino group of the first proline of N-degron is recognized by the carboxylate of Glu217 (β5) and the hydroxyl group of Tyr246 (β6). The carbonyl oxygen of the residue is coordinated with the side chain amide nitrogen of Gln89 (β1) and the hydroxyl group of Tyr246 (β6). Therefore, the side chain hydroxyl group of Tyr246 is a key determinant to recognize Nt-Pro1 by bipartate hydrogen bonds (Fig. 1E). The main chain nitrogen and oxygen atoms of the second Tyr2 residue form hydrogen bonds with the main chain oxygen and nitrogen atoms of Ser241 (L3). The side chain amide oxygen and nitrogen atoms of Gln270 (β8) form hydrogen bonds with the main chain nitrogen and oxygen atoms of the third Ile3 residue, respectively (Fig. 1E and F). Finally, the carbonyl oxygen of Gly239 (L3) interacts with the main chain nitrogen atom of the fourth Thr4 residue (Fig. 1E and F). The residues for recognizing the Pro/N-degron by hydrogen bonding interactions are absolutely conserved among yGid10, yGid4, and hGID4 (Fig. 2A). Interestingly, the atoms of the N-degron involved in the hydrogen bonds with Gid proteins are only main chain atoms, suggesting that the binding specificity must be from hydrophobic interactions.

3.4. Structural comparison with other GID N-recognins

Sequence alignment of yGid10 with yGid4 and hGID4 revealed that yGid10 and yGid4 share 39.66% sequence identity (55.17% similarity) with the β-barrel- and L1~L4-conjugated regions (Fig. 2A). yGid10 and hGID4 share 35.90% sequence identity (52.14% similarity) between the same regions. Meanwhile, AD shows only 10–16% sequence identity with each other. As noted above, the six key residues (Gln89, Glu217, Gly239, Ser241, Tyr246, and Gln270) forming the Pro/N-degron binding pocket are strictly conserved (Fig. 2A and 1E). The L5 loop of hGID4 is relatively shorter (4 residues) than that of yGid10 (12 residues) and yGid4 (11 residues) (Fig. 2A). This L5 loop faces yGid5, which acts as an adaptor for yGid4 and yGid10 [16,18], and thus, it seems that the extended L5 loop is specific for yeast proteins.

To further investigate the structural features, we superposed the structure of yGid10 with that of yGid4 (PDB ID: 7N53 chain-E) and hGID4 (PDB ID: 6CDC chain-A). yGid10 has two α-helices (α1 and α2) in AD, and the α2 of yGid10 corresponds to the α1-helix of hGID4 and yGid4 (Fig. 2B). yGid4 has an additional 35 amino acid residues (N239~F273) between the α2- and α3-helices, and structural information of the region is not yet available due to its flexible nature. This characteristic insertion of yGid4 may confer a substrate preference distinct from yGid10.

It has been reported that N-degron binding induces a conformational change in apo-Gid4 proteins, and the L3 loop shows the most dynamic movement [18,20,27]. Similarly, the L3 loop of yGid10 moves toward the N-degron binding site, and the Ser241 and Gly239 residues interact with the second and fourth residues of the substrate, respectively (Fig. 2C). Indeed, the L3 loop of yGid10 (23 residues) is exceptionally longer than that of yGid4 (16 residues) and hGID4 (15 residues) (Fig. 2A and C). Therefore, it seems that the longer L3 loop of yGid10 plays a role in substrate preference. The L4 loop of Gid4 proteins undergoes conformational

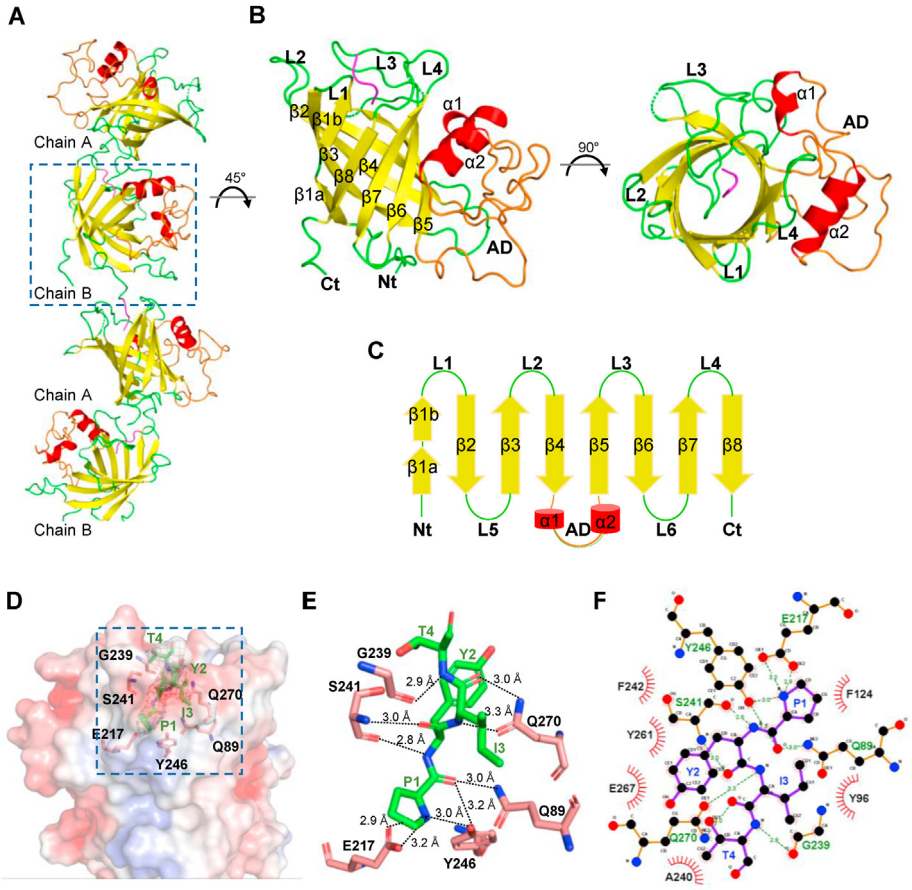

Fig. 1. Structural analysis of yeast Gid10 in complex with Pro/N-degron.
(**A**) Crystal packing representation of PYIT-tagged Gid10. The α-helices, β-strands, loops, and N-degron residues are colored red, yellow, green, and magenta, respectively. Each chain recognizes the N-terminal PYIT residues of the neighboring molecule. (**B**) The overall structure of yGid10. The α-helices (α1 and α2), β-strands (β1-β8), and connecting loops (L1-L4 for the substate binding side and L5-L6 for the opposite side) are numbered. The N- and C-termini are indicated as Nt and Ct, respectively. Accessary domain denoted as AD. (**C**) A schematic diagram of yGid10 topology. (**D**) A transparent molecular surface with electrostatic potentials shows the distribution of positively and negatively charged surfaces colored blue and red, respectively. Six key residues of yGid10 recognizing the N-degron peptide (green stick model) are shown in salmon and labeled. The 2Fo−Fc electron density map of the substrate peptide contoured at the 1.0-σ level is shown in the gray mesh. The substrate interaction region is indicated with a blue dashed box. (**E**) A close-up view of the substrate-binding site in the complex structure of yGid10-PYIT. The hydrogen bonds are denoted as black dashed lines with distances. (**F**) A schematic diagram showing the interactions between yGid10 and the PYIT peptide. The hydrogen bond interactions are shown as green dashed lines with distances, and hydrophobic interactions are indicated by red starbursts. (For interpretation of the references to color in this figure legend, the reader is referred to the Web version of this article.)

changes to tighten substrate binding upon complex formation [20]. Notably, the L4 loop and β8-strand in yGid4 have a dynamic conformational feature. Comparing apo-yGid4 (PDB ID: 6WSY chain E) and yGid4-PLT (PDB ID:7NS3 chain E), it has been identified that the breakage of the β1-strand (Thr130-Tyr132) splits into two short strands (β1a and β1b). Thus, it weakens the hydrogen bonding interactions between the β1- and β8-strands to allow the structural transition at the tip of the β8-strand (Fig. 2D). The glutamine residue (Gln270 in yGid10 and Gln340 in yGid4) at the β8-strand moves upward to accommodate the third residue of N-degron (Fig. 2D). The side chain of Gln270 is critical for recognition of the peptide bond of the third residue of the N-degron (Fig. 1E). However, there was no such conformational change in hGID4 upon complex formation [20] (Fig. 2D).

3.5. Substrate selectivity of yGid10

yGid10, yGid4, and hGID4 recognize the same Nt-Pro residue but show distinct specificities [12,17,19,20]. Especially at the second position of the Pro/N-degron, yGid4 prefers small and/or polar residues, and hGID4 shows some stringency to the Gly residue. However, yGid10 showed promiscuous recognition of a wide range of hydrophobic residues from small to bulky side chains. All these N-recognins prefer hydrophobic residues at the third and fourth positions of Pro/N-degron. To investigate the reason for this selectivity, we compared the accommodating region of the N-degron in the GID proteins. As described above, there is no particular polar interaction for specificity, and thus, the hydrophobic surface properties were compared (Fig. 3). The hole accommodating Nt-Pro in the three N-recognins shares a similar hydrophobic property (Fig. 3A). It has been reported that these N-recognins also recognize nonproline Nt-residues, initially in yGid10 [17] and then hGID4 [19] and very recently in yGid4 [28]. These nonproline Nt-residues are all hydrophobic residues and are clearly explained by the nonpolar nature of this hole.

All four loops (L1-L4) of GID N-recognins efficiently collaborate in the binding of Pro/N-degron (Fig. 1B). In contrast to the Gid4 proteins, the loops of yGid10 are longer and flexible for generating a larger binding pocket, mainly due to the L3 loop (Fig. 2C). The L4 loop recognizes the second residue of N-degron, and therefore, it is inferred that the selectivity originates from the characteristics of amino acids composed of the L4 loop. Compared with the sequence of the L4 loop of yGid4 and hGID4, that of yGid10 possesses more hydrophobic residues (Fig. 2A) for energetically favorable

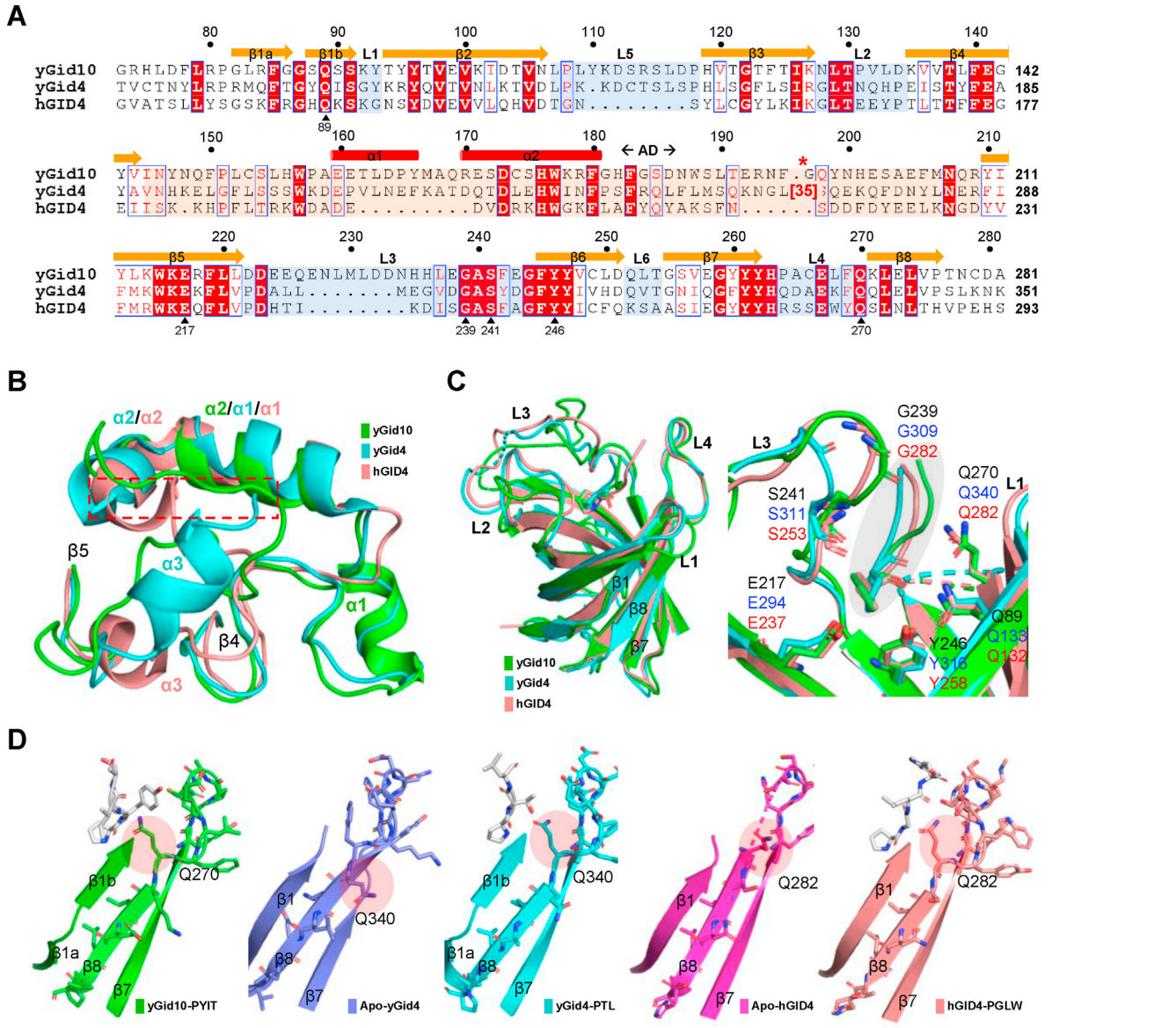

Fig. 2. Structural comparison of yGid10 with yGid4 and hGID4.
(**A**) Sequence alignment of Gid proteins. Thirty-five residues (N239–F273) of yGid4 are omitted for clarity and indicated as a red * symbol [35]. Connecting loop regions and AD are shaded in gray and salmon, respectively. (**B**) Superposition of accessory domains. yGid10, yGid4, and hGID4 are colored green, cyan, and salmon, respectively. The red dashed box represents the region of yGid4, which is not a structurally determined region of yGid4. (**C**) A superposition of the structure of the yGid10-PYIT complex with those of yGid4 from the Gid^{SR4} complex and hGID4-PSRW complex. The color scheme is the same as Panel (B). Residues of yGid10 are labeled in black, and each equivalent residue of yGid4 and hGID4 is labeled in blue and red, respectively. A transparent gray oval indicates the bound N-degron peptide region. (**D**) Structural shift of the β8-strand in yGid10 and yGid4 upon complex formation with the N-degron peptide. yGid10-PYIT, apo-yGid4, yGid4-PLT, apo-hGID4, and hGID4-PGLW are colored green, slate, cyan, magenta, and salmon, respectively. The bound N-degron peptides are shown in stick models colored white. Transparent reddish circles indicate the Q270 of yGid10 and its equivalent residues in yGid4 and hGID4. (For interpretation of the references to color in this figure legend, the reader is referred to the Web version of this article.)

environments (Fig. 3B). Furthermore, yGid10 generates a larger pocket for the bulky tyrosyl side chain at the second position than that for Thr in yGid4 and that for Gly in hGID4 (Fig. 3B). The corresponding hydrophobic region in the L4 loop of yGid10 is partly hydrophilic in yGid4 and hGID4 (the upper right corner of Fig. 3B). Consistent with the results obtained from the phage-display peptide library screen, yGid4 and hGID4 favor Asp at the second position, whereas yGid10 favors Trp [28]. There is a conserved hydrophobic patch near the binding site of the third residue of N-degron (Fig. 3B). It can be clearly explained that the preference of the third position of the N-degron is also hydrophobic residues [28].

Intriguingly, a natural substrate of yGid10 N-recognin was very recently identified [29]. yGid10-containing GID complex ubiquitinates the α-arrestin Art2, which regulates the endocytosis of plasma membrane nutrient transporters. Fortuitously, the Nt-sequence of Art2 is Nt-Pro-Phe-Ile-Thr-Ser-Arg-Pro-Val [29], which is almost identical to our designed sequence Nt-Pro-Tyr-Ile-Thr-Val by modification of the original sequence Nt-Met-Tyr-Ile-Thr-Val obtained from a yeast-two-hybrid screen [17]. Therefore, the current structure of yGid10 in complex with the Pro/N-degron, which is nearly identical to the natural substrate, broadens our understanding of the structural diversity and substrate specificity of recognition components in the GID E3 Ub ligase complex.

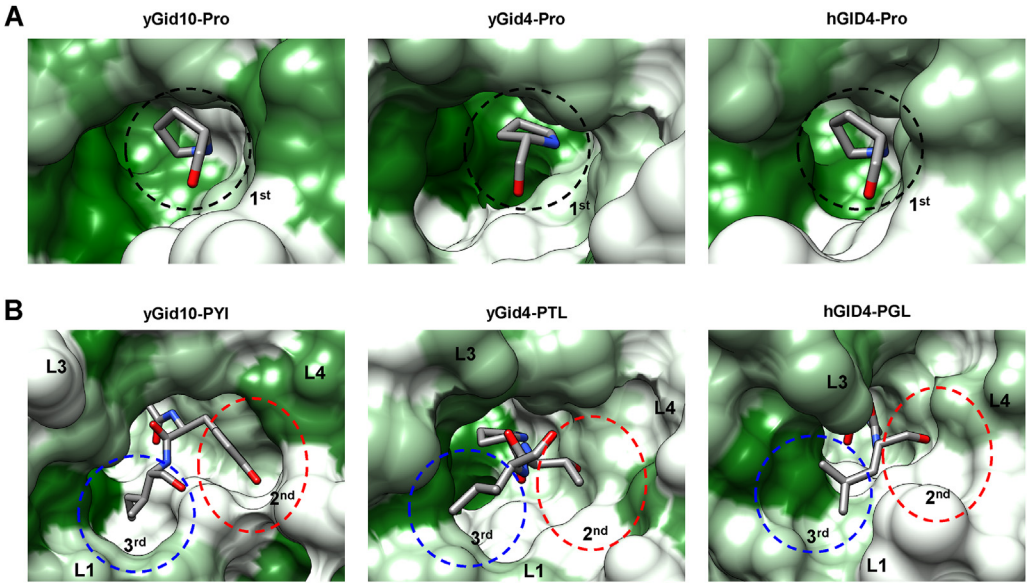

Fig. 3. The hydrophobic pocket of the recognition components of GID E3 ubiquitin ligase.
(**A**) The primary proline recognition regions of yGid10-PYIT, yGid4-PTL, and hGID4-PGLW were compared. Only the N-terminal proline of substrate peptides is shown for clarity. (**B**) The recognition regions of the side chain atoms of the 2nd and 3rd residues of Pro/N-degron are shown in red and blue dashed circles, respectively. Hydrophobicity increases as the surface color changes from white to green. (For interpretation of the references to color in this figure legend, the reader is referred to the Web version of this article.)

Declaration of competing interest

The authors declare no conflicts of interest.

Acknowledgments

We thank the staff at beamlines 5C and 11C at the Pohang Accelerator Laboratory, Korea. This research was supported by the Basic Science Research Program through the National Research Foundation of Korea (NRF) funded by the Korean government (2021R1A6A3A01088067 to J.S.S.; 2020R1A2C3008285 and 2020R1A5A1019023 to H.K.S.). This work was also partially supported by the Korea University Grant.

Appendix A. Supplementary data

Supplementary data to this article can be found online at https://doi.org/10.1016/j.bbrc.2021.10.007.

References

[1] A. Hershko, A. Ciechanover, The ubiquitin system for protein degradation, Annu. Rev. Biochem. 61 (1992) 761–807, https://doi.org/10.1146/annurev.bi.61.070192.003553.
[2] A. Varshavsky, The ubiquitin system, autophagy, and regulated protein degradation, Annu. Rev. Biochem. 86 (2017) 123–128, https://doi.org/10.1146/annurev-biochem-061516-044859.
[3] A. Varshavsky, The ubiquitin system, an immense realm, Annu. Rev. Biochem. 81 (2012) 167–176, https://doi.org/10.1146/annurev-biochem-051910-094049.
[4] W. Baumeister, A. Lupas, The proteasome, Curr. Opin. Struct. Biol. 7 (1997) 273–278, https://doi.org/10.1016/s0959-440x(97)80036-x.
[5] M. Scheffner, U. Nuber, J.M. Huibregtse, Protein ubiquitination involving an E1-E2-E3 enzyme ubiquitin thioester cascade, Nature 373 (1995) 81–83, https://doi.org/10.1038/373081a0.
[6] A. Varshavsky, N-degron and C-degron pathways of protein degradation, Proc. Natl. Acad. Sci. U.S.A. 116 (2019) 358–366, https://doi.org/10.1073/pnas.1816596116.
[7] W.S. Choi, B.C. Jeong, Y.J. Joo, M.R. Lee, J. Kim, M.J. Eck, H.K. Song, Structural basis for the recognition of N-end rule substrates by the UBR box of ubiquitin ligases, Nat. Struct. Mol. Biol. 17 (2010) 1175–1181, https://doi.org/10.1038/nsmb.1907.
[8] M.K. Kim, S.J. Oh, B.G. Lee, H.K. Song, Structural basis for dual specificity of yeast N-terminal amidase in the N-end rule pathway, Proc. Natl. Acad. Sci. U.S.A. 113 (2016) 12438–12443, https://doi.org/10.1073/pnas.1612620113.
[9] C.S. Hwang, A. Shemorry, A. Varshavsky, N-terminal acetylation of cellular proteins creates specific degradation signals, Science 327 (2010) 973–977, https://doi.org/10.1126/science.1183147.
[10] R.T. Timms, Z. Zhang, D.Y. Rhee, J.W. Harper, I. Koren, S.J. Elledge, A glycine-specific N-degron pathway mediates the quality control of protein N-myristoylation, Science 365 (2019), eaaw4912, https://doi.org/10.1126/science.aaw4912.
[11] J.M. Kim, O.H. Seok, S. Ju, J.E. Heo, J. Yeom, D.S. Kim, J.Y. Yoo, A. Varshavsky, C. Lee, C.S. Hwang, Formyl-methionine as an N-degron of a eukaryotic N-end rule pathway, Science 362 (2018), eaat0174, https://doi.org/10.1126/science.aat0174.
[12] S.J. Chen, X. Wu, B. Wadas, J.H. Oh, A. Varshavsky, An N-end rule pathway that recognizes proline and destroys gluconeogenic enzymes, Science 355 (2017), eaal3655, https://doi.org/10.1126/science.aal3655.
[13] S.M. Schork, G. Bee, M. Thumm, D.H. Wolf, Catabolite inactivation of fructose-1,6-bisphosphatase in yeast is mediated by the proteasome, FEBS Lett. 349 (1994) 270–274, https://doi.org/10.1016/0014-5793(94)00668-7.
[14] S.M. Schork, M. Thumm, D.H. Wolf, Catabolite inactivation of fructose-1,6-bisphosphatase of saccharomyces-cerevisiae - degradation occurs via the ubiquitin pathway, J. Biol. Chem. 270 (1995) 26446–26450, https://doi.org/10.1074/jbc.270.44.26446.
[15] M. Hammerle, J. Bauer, M. Rose, A. Szallies, M. Thumm, S. Dusterhus, D. Mecke, K.D. Entian, D.H. Wolf, Proteins of newly isolated mutants and the amino-terminal proline are essential for ubiquitin-proteasome-catalyzed catabolite degradation of fructose-1,6-bisphosphatase of Saccharomyces cerevisiae, J. Biol. Chem. 273 (1998) 25000–25005, https://doi.org/10.1074/jbc.273.39.25000.
[16] R. Menssen, J. Schweiggert, J. Schreiner, D. Kusevic, J. Reuther, B. Braun, D.H. Wolf, Exploring the topology of the Gid complex, the E3 ubiquitin ligase involved in catabolite-induced degradation of gluconeogenic enzymes, J. Biol. Chem. 287 (2012) 25602–25614, https://doi.org/10.1074/jbc.M112.363762.
[17] A. Melnykov, S.J. Chen, A. Varshavsky, Gid10 as an alternative N-recognin of the Pro/N-degron pathway, Proc. Natl. Acad. Sci. U.S.A. 116 (2019) 15914–15923, https://doi.org/10.1073/pnas.1908304116.
[18] S. Qiao, C.R. Langlois, J. Chrustowicz, D. Sherpa, O. Karayel, F.M. Hansen, V. Beier, S. von Gronau, D. Bollschweiler, T. Schafer, A.F. Alpi, M. Mann, J.R. Prabu, B.A. Schulman, Interconversion between anticipatory and active GID E3 ubiquitin ligase conformations via metabolically driven substrate receptor assembly, Mol. Cell 77 (2020) 150–163, https://doi.org/10.1016/j.molcel.2019.10.009.
[19] C. Dong, S.J. Chen, A. Melnykov, S. Weirich, K. Sun, A. Jeltsch, A. Varshavsky, J. Min, Recognition of nonproline N-terminal residues by the Pro/N-degron pathway, Proc. Natl. Acad. Sci. U.S.A. 117 (2020) 14158–14167, https://doi.org/10.1073/pnas.2007085117.
[20] C. Dong, H. Zhang, L. Li, W. Tempel, P. Loppnau, J. Min, Molecular basis of GID4-mediated recognition of degrons for the Pro/N-end rule pathway, Nat. Chem. Biol. 14 (2018) 466–473, https://doi.org/10.1038/s41589-018-0036-1.

[21] A.J. McCoy, R.W. Grosse-Kunstleve, P.D. Adams, M.D. Winn, L.C. Storoni, R.J. Read, Phaser crystallographic software, J. Appl. Crystallogr. 40 (2007) 658–674, https://doi.org/10.1107/S0021889807021206.
[22] A. Casanal, B. Lohkamp, P. Emsley, Current developments in Coot for macromolecular model building of electron cryo-microscopy and crystallographic data, Protein Sci. 29 (2020) 1069–1078, https://doi.org/10.1002/pro.3791.
[23] E.F. Pettersen, T.D. Goddard, C.C. Huang, E.C. Meng, G.S. Couch, T.I. Croll, J.H. Morris, T.E. Ferrin, UCSF ChimeraX: structure visualization for researchers, educators, and developers, Protein Sci. 30 (2021) 70–82, https://doi.org/10.1002/pro.3943.
[24] L. Kim, D.H. Kwon, J. Heo, M.R. Park, H.K. Song, Use of the LC3B-fusion technique for biochemical and structural studies of proteins involved in the N-degron pathway, J. Biol. Chem. 295 (2020) 2590–2600, https://doi.org/10.1074/jbc.RA119.010912.
[25] P.T. Wingfield, N-terminal methionine processing, Curr. Protein Pept. Sci. 88 (2017) 6.14.1–16.14.3, https://doi.org/10.1002/cpps.29.
[26] S.J. Chen, L. Kim, H.K. Song, A. Varshavsky, Aminopeptidases trim Xaa-Pro proteins, initiating their degradation by the Pro/N-degron pathway, Proc. Natl. Acad. Sci. U.S.A. 118 (2021), e2115430118, https://doi.org/10.1073/pnas.2115430118.
[27] D. Sherpa, J. Chrustowicz, S. Qiao, C.R. Langlois, L.A. Hehl, K.V. Gottemukkala, F.M. Hansen, O. Karayel, S. von Gronau, J.R. Prabu, M. Mann, A.F. Alpi, B.A. Schulman, GID E3 ligase supramolecular chelate assembly configures multipronged ubiquitin targeting of an oligomeric metabolic enzyme, Mol. Cell 81 (2021) 2445–2459, https://doi.org/10.1016/j.molcel.2021.03.025.
[28] J. Chrustowicz, D. Sherpa, J. Teyra, M.S. Loke, G. Popowicz, J. Basquin, M. Sattler, J.R. Prabu, S.S. Sidhu, B.A. Schulman, Multifaceted N-Degron Recognition and Ubiquitylation by GID/CTLH E3 Ligases, bioRxiv, 2021, https://doi.org/10.1101/2021.09.03.458554.
[29] C.R. Langlois, V. Beier, O. Karayel, J. Chrustowicz, D. Sherpa, M. Mann, B.A. Schulman, A GID E3 Ligase Assembly Ubiquitinates an Rsp5 E3 Adaptor and Regulates Plasma Membrane Transporters, bioRxiv, 2021, https://doi.org/10.1101/2021.09.02.458684.